Eur J Vasc Endovasc Surg (2015) 49, 33–38

Variability of Origin of Splanchnic and Renal Vessels From the Thoracoabdominal Aorta

D. Mazzaccaro *, **G. Malacrida, G. Nano**

Ist Unit of Vascular Surgery, IRCCS Policlinico San Donato, University of Milan, San Donato Milanese, Italy

WHAT THIS PAPER ADDS

To date, there are no studies in the literature that assess the anatomic variability of the origin of splanchnic and renal vessels. The clinical applicability of the study, although limited by the small number of samples tested, addresses the endovascular treatment of thoracoabdominal aneurysms using fenestrated or branched grafts. Currently, the main limitation of these techniques is the need to customize the graft to the anatomy of the individual patient. This study confirms the feasibility of design of endografts with standard fenestrations for the celiac trunk and the superior mesenteric artery; however, the main concern is for the anatomical variability of the renal vessels.

Objective: To analyze the variability of origin of the celiac trunk (CT), the superior mesenteric artery (SMA), the right renal artery (RRA), and the left renal artery (LRA) in terms of mutual distances, angle from the sagittal aortic axis (clock position), and ostial diameters on computed tomography angiographies (CTAs) in three groups of patients.

Methods: One hundred and fifty CTAs of 50 patients with a non-dilated thoracoabdominal aorta (group A), 50 with thoracoabdominal aneurysm (B), and 50 with infrarenal aneurysm (C) were reviewed. The measurements performed on CTAs, as well as the patients' age, sex, and body surface area, were analyzed. p values $<.05$ were considered statistically significant.

Results: The clock position of the CT and the SMA, the diameters of all vessels, and the distance of the CT–SMA followed a Gaussian distribution. In contrast, the clock position of the renal vessels did not follow a normal distribution, and nor did the distances of the SMA–RRA, SMA–LRA, RRA–LRA or the distances between the renal arteries and the aortic bifurcation. The same values did not differ significantly among the three groups, with the exception of the distances between the renal arteries and the aortic bifurcation, significantly greater in group C. The clock position of the LRA and the distances of the SMA–LRA, SMA–RRA, RRA–LRA and between both renal arteries and the aortic bifurcation showed a significant correlation with the increase of aortic diameter.

Conclusion: The anatomic variability of the origin of both the CT and the SMA in terms of clock position and mutual distances followed a Gaussian distribution, regardless of group. The same applies to the ostial diameters of renal and visceral vessels. In contrast, the origin of the renal vessels had a statistically significant heterogeneity that seemed to be correlated with the increase of aortic diameter in the mesenteric and renal aortic region.

Article history: Received 10 August 2014, Accepted 7 October 2014, Available online 10 November 2014

Keywords: Anatomy, Endovascular, Thoracoabdominal aneurysm

INTRODUCTION

In recent years the development of new techniques, together with improvements in materials, has progressed from overcoming the anatomic limits for the endovascular treatment of infrarenal abdominal aortic aneurysms (AAA), to the challenging treatment of more complex juxtarenal, pararenal, or even thoracoabdominal aortic aneurysms (TAAAs).[1]

Endovascular treatment of this type of aneurysm requires a different approach when compared with the treatment of either infrarenal or thoracic aneurysms. It encompasses not only the importance of having anatomic areas suitable for correct sealing of the graft, but also the need to preserve perfusion of visceral and renal vessels.

Therefore, endoprostheses with fenestrations or branches to preserve visceral and/or renal perfusion, and to ensure complete exclusion of the aortic pathology have been developed. Many studies have reported on the use of these devices and have demonstrated efficacy with a good safety profile, and low rates of peri-operative morbidity and mortality.[2]

* Corresponding author.

E-mail address: danymazzak83@libero.it (D. Mazzaccaro).

1078-5884/$ – see front matter

http://dx.doi.org/10.1016/j.ejvs.2014.10.005

Currently, however, the main limitations of these grafts are their high cost and lack of availability in an emergency setting, because of the need to customize the graft to the anatomy of the individual patient.

These limits might be overcome by the development of endografts with "standard" fenestrations adaptable to most anatomies, reserving customization to cases that differ from these anatomical models.

In light of this, the aim of this study was to test the hypothesis that in the general population the anatomic variability of visceral and renal vessels emerging from the aorta in terms of mutual distances, ostial diameters, and angle of origin from the sagittal aortic axis follows a Gaussian pattern and can be predicted within set parameters.

MATERIALS AND METHODS

Measurements on computed tomography angiography

Computed tomography angiograms (CTAs) of the thoracoabdominal aorta were examined in a retrospective fashion in three groups of patients. The first group (group A) had no dilatation of the thoracoabdominal aorta; the second group (group B) had dilatation involving both the splanchnic and renal vessels; and the third group (group C) had dilatation of the infrarenal abdominal aorta beginning at least 15 mm beyond the origin of the lower renal artery.

Dilatation was defined as an increase of the aortic diameter of at least 50% compared with an adjacent segment.

To facilitate the study, CTAs that demonstrated variations of the origin of visceral vessels or the presence of accessory renal arteries were excluded from the analysis (five and four CTAs, respectively). All analyzed CTAs were performed from 2012 onwards, with 1 mm slices. These images were analyzed using dedicated software (3mensio Vascular™; 3mensio Medical Imaging BV, Bilthoven, the Netherlands).

The workstation for analysis of CTAs was three dimensional. Using multiplanar reconstructions, the antero-posterior, cranio-caudal, and latero-lateral anatomy of the aorta and its vessels could be reconstructed. From these data, the reconstruction software automatically built the centerline (i.e., the line that ideally passes through the center of the aortic lumen) and made the curved planar reconstruction (CPR), the axis of which was perpendicular to the centerline. Thanks to the CPR an accurate calculation of distances and angles could be performed, minimizing any error.

Moreover the use of maximum intensity projection images contributed to the accurate quantification of calcification in the aortic neck.

Examination of the CTA images was carried out to identify the ostial center of the visceral (celiac trunk [CT] and superior mesenteric artery [SMA]) and renal vessels (right renal artery [RRA] and left renal artery [LRA]). At the same level the aortic diameters (antero-posterior and latero-lateral), the angle of the origin of the vessels relative to the sagittal aortic axis (clock position), and the ostial diameters of the vessels were measured. The mutual distances between the centers of origin of the vessels were also measured, as well as the distance between the renal arteries and the aortic bifurcation. When distances were measured, antero-posterior and latero-lateral aortic diameters were recorded at their maximum level.

All measurements were entered into a database, along with the age of the patient (the difference between the date of execution of the CTA and date of birth), patient sex and the body surface area (BSA) calculated: $[(\text{height (cm)} \times \text{weight (kg)}/3600]^{1/2}$.

Statistical analysis

Data were analyzed using JMP 5.1.2 (SAS Institute, Cary, NC, USA).

In particular, the normality of the distribution of the different variables was tested using the Shapiro—Wilk test.

Data are expressed as mean $\pm$ SD with 95% confidence intervals. When expressed as median, the interquartile range (IQR) is indicated.

The comparison of variables with normal distribution was performed by a two-tailed Student *t* test, while the comparison of non-parametric variables was performed using the chi-square and Wilcoxon tests. Correlations were made using simple logistic regression.

A p value $<.05$ was considered statistically significant.

RESULTS

150 CTAs were examined. The median age of the patients was 74.3 years (IQR 67.5—80.1). Fifty patients did not have any dilatation of the thoracoabdominal aorta (group A), 50 had thoracoabdominal aortic dilatation (group B), and 50 had infrarenal aortic dilatation (group C). The three groups differed for median age, which was significantly lower in group A compared with both groups B and C, being, respectively, 68.7 years (IQR 57.5—77.3), 74 (IQR 68.1—80.2), and 76.4 (IQR 71.7—81.3) ($p = .01$). Women were more numerous in group A (40%) than in the remaining two groups (14% and 18% for groups B and C, respectively; $p < .01$).

The median diameter of the aorta was 45.2 mm (IQR 39.2—53.8 mm) in group B and 55 mm (IQR 48.0—59.0 mm) in group C. In group B the Crawford classification was 36 type IV, eight type III, four type II, and two type I.

Regardless of the group, the normal distribution of all measurements was tested. As reported in Table 1, the clock position of both the CT and the SMA (Fig. 1), the diameters at the origin of the latter and of both renal arteries, as well as the distance between the CT and the SMA followed a Gaussian distribution. In contrast, the clock position of the renal vessels did not follow a normal distribution (Fig. 2), and nor did the distances between the SMA and both renal arteries, the mutual distances between the two renal arteries, or the distances between the renal vessels and the aortic bifurcation. Furthermore, in 55.3% of cases the RRA arose at a more cranial level than the LRA and in 27.3% of cases at the same level.

Table 1. Distribution of measurements on computed tomography angiograms.

		Mean ± SD	95% CI	*p*
CT angle		21.5 ± 6.5	18.8–24.1	.80
CT diameter		7.3 ± 1.2	7.1–7.5	.10
SMA angle		12.3 ± 1.3	10.5–14.1	.06
SMA diameter		7.5 ± 1.3	7.2–7.7	.20
RRA angle		−52.9 ± 26.1	−57.1 to −48.6	<.01
RRA diameter		5.4 ± 1.2	5.2–5.6	.10
LRA angle		89.5 ± 20.2	86.3–92.8	<.01
LRA diameter		5.2 ± 0.9	5.0–5.4	.20
Distances	CT–SMA	15.5 ± 5.8	14.5–16.4	.80
	SMA–RRA	14.8 ± 8.1	13.4–16.1	<.01
	SMA–LRA	18.1 ± 7.9	16.7–19.3	<.01
	RRA–LRA	7.1 ± 7.4	5.8–8.2	<.01
	RRA–Bif	101.6 ± 19.2	98.5–104.7	<.01
	LRA–Bif	98.7 ± 20.1	95.5–102	<.01

Note. $p < .05$ indicates a non-Gaussian distribution of the measurements. The measurements of the diameters and distances are expressed in mm and angles in degrees. CI = confidence interval; CT = celiac trunk; SMA = superior mesenteric artery; RRA = right renal artery; LRA = left renal artery; Bif = aortic bifurcation.

The subgroup analysis showed that all measurements in group A did not differ significantly compared with subjects with dilated aortas either in the thoracoabdominal or in the infrarenal aorta, with the exception of the distances between both the renal arteries and aortic bifurcation, which were significantly higher in patients with infrarenal aortic dilatation (both $p < .01$) (Table 2).

Finally, the clock position of the CT, the SMA, RRA, the diameter at the origin of all vessels, and the distance between the CT and the SMA did not show any statistical correlation with the antero-posterior or latero-lateral maximum aortic diameters, nor with patients' age, sex or BSA. In contrast, the clock position of the LRA and the distances between the SMA–LRA, SMA–RRA, LRA–RRA, LRA–aortic bifurcation, and RRA–aortic bifurcation correlated significantly with the antero-posterior and latero-lateral aortic diameters (Table 3).

DISCUSSION

It is evident from the literature that complications after surgery for a TAAA are potentially devastating and have a multifactorial etiology.[3] Even in centers of excellence they occur frequently despite numerous strategies aimed at reducing these risks. The same centers have highlighted the need to approach the treatment of this type of pathology in a less invasive way, as has occurred for the thoracic and abdominal aorta.

Currently, there are multiple endovascular solutions for the treatment of TAAA. There are some reports of the use of the chimney and periscope techniques. It is applicable in a variety of clinical situations using readily available materials, with a high degree of technical success and very low surgical conversion rates.[4] However, one of the main concerns is type Ia endoleak, which is reported more frequently than after a conventional endovascular abdominal aortic repair owing to the presence of "gutters" around the Chimney stent,[5] which reflect the degree of conformability that the aortic stent graft can undergo to accommodate the insertion of the stent between it and the native aortic wall.

For the present and foreseeable future it is the use of fenestrated or branched stentgrafts, which exemplify the continuous development of the technology that is driving the practice of vascular surgery. The concept underlying the use of fenestrated endografts is the careful analysis of the aortic anatomy, which allows for the precise design of the fenestrations for the visceral and renal vessels in the graft. However, the personalized nature of such devices often requires weeks of processing and packaging, which leads to an increase in costs, a delay in the treatment of patients, and precludes the treatment of acute aortic pathologies.

It is for these reasons that many groups are currently working towards the development of "off the shelf" devices.

These grafts must be able to adapt to a significant portion of patients for whom they are designed, without significantly increasing the risks associated with the repair. For the treatment of juxta- and pararenal aneurysms, two devices are currently under study. The first is the p-Branch Cook Zenith device (Cook, Bloomington, IN, USA), which has a fixed hole for the SMA, a large scallop for the CT, and two flexible fenestrations for the location of the renal arteries. The other device still under evaluation is the Ventana (Endologix Inc., Irvine, CA, USA), designed with a large scallop for the CT and the SMA, and two fenestrations for

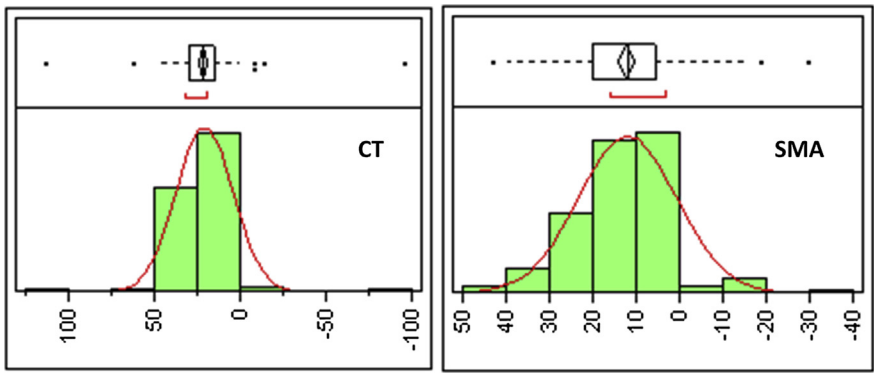

Figure 1. Gaussian distribution of the clock position of the celiac trunk (CT; on the left) and superior mesenteric artery (SMA; on the right). Numbers on the abscissa axis indicate the angle in degrees.

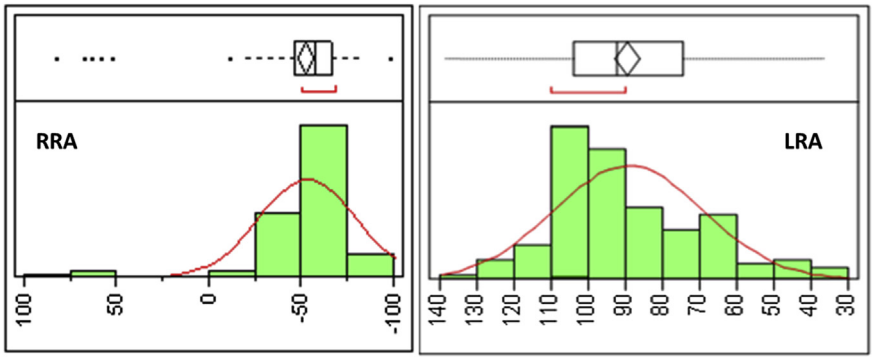

Figure 2. Non-Gaussian distribution of clock position of right renal artery (RRA; on the left) and left renal artery (LRA; on the right). Numbers on the abscissa axis indicate the angle in degrees.

the renal arteries, with positioning flexibility given by the redundancy of the tissue in the central part, which is not connected to the stent.

Given the incentive to design endoprostheses that can be adapted to most patients, the question arises whether one can speak of a "standard aortic anatomy".

Sobocinski et al. evaluated a total of 100 patients with juxtarenal and/or pararenal aortic aneurysms who underwent endovascular treatment with custom made fenestrated designs to determine the feasibility of the same cases for off the shelf options.[6] Surprisingly, 72.0% of patients had an anatomy suitable for a "standard" fenestrated approach. In the remaining patients, the primary cause of non-feasibility was the RRA, the origin of which did not correspond to the position of its respective fenestration. This feasibility percentage seems slightly high and it was probably due to the pre-selection of patients for the endovascular treatment to which they were subjected.

For aneurysms with complex thoracoabdominal involvement, the only "off the shelf" device is currently the t-Branch Zenith Cook. Similar to Sobocinski et al.,[6] Bisdas et al. retrospectively analyzed the clinical and radiological data of 43 consecutive patients with TAAA treated with a multi-branched custom made graft between June 2008 and February 2013 in order to determine suitability for treatment with the t-Branch system.[7] An analysis of the results showed that 49.0% of patients were suitable for treatment with that device and a further 14.0% would have been suitable with additional procedures (e.g., thoracic endografting with or without a left carotid-subclavian bypass). Also in this report the main cause of non-feasibility in the remaining 37.0% of cases was the variability of the origin of the renal arteries in terms of distance to the CT, cranio-caudal orientation, and distance to the aortic bifurcation.

The results of the present study are comparable with these data. In particular, the present study confirms the anatomic homogeneity of the origin of both the celiac artery and the SMA, regardless of factors such as the aortic diameter, age, sex, or BSA. As reported in the studies of Sobocinski et al. and Bisdas et al.,[6,7] the main limitation to the "standardization" of the aortic anatomy in the present study was the renal arteries, the angles of origin of which (mostly for the LRA) and mutual distances between them and the SMA, and aortic bifurcation increased with the increase of aortic diameter. It is quite intuitive that the more the aortic diameters were dilated, the more the distances between the arteries was enlarged. The fact that the renal arteries are more susceptible to this phenomenon reflects

Table 2. Differences among groups.

		Group A	Group B	Group C	*p*
CT angle		23.3 (18.6—29.3)	19.3 (10.6—27.8)	22.3 (15.7—29.4)	.19
CT diameter		7.2 (6.5—8.0)	7.1 (6.7—8.1)	7.4 (6.5—8.3)	.83
SMA angle		15.1 (8.2—21.4)	9.7 (3.4—18.5)	12.0 (5.9—23.0)	.06
SMA diameter		7.3 (6.8—8.1)	7.2 (6.6—7.9)	7.0 (6.2—8.4)	.52
RRA angle		−51.8 (−63.7 to −41.8)	−60.2 (−67.5 to −46.5)	−59.1 (−67.2 to −50.3)	.19
RRA diameter		5.4 (4.9—6.2)	5.3 (4.7—6.0)	5.1 (4.3—6.5)	.52
LRA angle		100.1 (86.8—105.5)	87.8 (70.1—99.8)	92.8 (72.8—106.7)	.06
LRA diameter		5.4 (4.8—6.3)	5.4 (4.9—6.3)	5.2 (4.5—6.2)	.56
Distances	CT—SMA	15.0 (12.0—20.0)	15.0 (10.0—20.0)	15.0 (10.7—18.2)	.75
	SMA—RRA	12.2 (8.2—16.2)	15.0 (10.0—21.0)	15.0 (10.0—19.2)	.08
	SMA—LRA	15.0 (11.2—20.0)	17.5 (12.0—24.2)	18.4 (12.9—25.0)	.45
	RRA—LRA	5.0 (0—10.0)	6.6 (0.7—10.6)	5.0 (0—7.8)	.33
	RRA—Bif	91.2 (85.0—100.3)	101.0 (90.0—115.0)	113.5 (102.6—122.0)	**<.01**
	LRA—Bif	90.0 (81.0—97.5)	100.0 (85.0—119.2)	108.4 (95.0—120.2)	**<.01**

Note. Values are expressed as median (interquartile range). Distances in mm, angles in degrees. Significant *p* values are in bold. CT = celiac trunk; SMA = superior mesenteric artery; RRA = right renal artery; LRA = left renal artery; Bif = aortic bifurcation.

Table 3. Correlations of measures with aortic diameters, sex, age and body surface area (BSA).

		r^2	p
CT angle	Aortic diameter AP	.01	.33
	Aortic diameter LL	.02	.16
	Age	<.01	.94
	BSA	<.01	.62
	Sex	n.a.	.13
CT diameter	Aortic diameter AP	.01	.36
	Aortic diameter LL	.02	.26
	Age	.01	.99
	BSA	<.01	.53
	Sex	n.a.	.70
SMA angle	Aortic diameter AP	.02	.13
	Aortic diameter LL	.02	.11
	Age	<.01	.61
	BSA	.01	.37
	Sex	n.a.	.50
SMA diameter	Aortic diameter AP	<.01	.06
	Aortic diameter LL	<.01	.76
	Age	<.01	.59
	BSA	<.01	.87
	Sex	n.a.	.58
RRA angle	Aortic diameter AP	.01	.23
	Aortic diameter LL	.01	.31
	Age	<.01	.57
	BSA	<.01	.71
	Sex	n.a.	.26
RRA diameter	Aortic diameter AP	.10	.47
	Aortic diameter LL	<.01	.58
	Age	<.01	.59
	BSA	<.01	.87
	Sex	n.a.	.58
LRA angle	Aortic diameter AP	.13	**<.01**
	Aortic diameter LL	.14	**<.01**
	Age	.02	.18
	BSA	<.01	.70
	Sex	n.a.	.90
LRA diameter	Aortic diameter AP	<.01	.82
	Aortic diameter LL	<.01	.86
	Age	.02	.12
	BSA	<.01	.87
	Sex	n.a.	.46
CT—SMA distance	Aortic diameter AP[a]	.05	.20
	Aortic diameter LL[a]	.04	.40
	Age	.02	.20
	BSA	.01	.43
	Sex	n.a.	.21
SMA—RRA distance	Aortic diameter AP[a]	.08	**.01**
	Aortic diameter LL[a]	.07	**<.01**
	Age	.02	.11
	BSA	.02	.11
	Sex	n.a.	.15
SMA—LRA distance	Aortic diameter AP[a]	.06	**.01**
	Aortic diameter LL[a]	.04	**.04**
	Age	.02	.13
	BSA	<.01	.92
	Sex	n.a.	.74
RRA—LRA distance	Aortic diameter AP[a]	.09	**<.01**
	Aortic diameter LL[a]	.07	**<.01**
	Age	.01	.44
	BSA	<.01	.94
	Sex	n.a.	.68
RRA—bif distance	Aortic diameter AP[a]	.09	**<.01**
	Aortic diameter LL[a]	.09	**<.01**
	Age	.02	.12
	BSA	<.01	.51
	Sex	n.a.	.30
LRA—bif distance	Aortic diameter AP[a]	.09	**<.01**
	Aortic diameter LL[a]	.13	**<.01**
	Age	<.01	.34
	BSA	<.01	.92
	Sex	n.a.	0.40

Note. Significant p values are in bold. CT = celiac trunk; SMA = superior mesenteric artery; RRA = right renal artery; LRA = left renal artery; bif = aortic bifurcation; AP = antero-posterior; LL = latero-lateral; n.a. = not applicable.

[a] Greatest measurement in the nearby region.

the absence of anatomical fixation of these vessels, differing from the relation of the CT to the SMA, which is not influenced by the aortic dilatation near their origins. Moreover, in this area the aorta is extensively fixed by the diaphragm.

Some recent papers have reported the use of dynamic CTA in the evaluation of changes in aortic conformation during the cardiac cycle.[8,9] In these studies, the existence of an axial aortic pulsatility was evident. Moreover, Iezzi and Coll reported the existence of a longitudinal aortic pulsatility during the cardiac cycle for the infrarenal abdominal aorta, from the lowest renal artery to the aortic bifurcation,[10] which could possibly explain, in part, some of the findings of this study. The conclusions are limited by the small number of samples tested. Moreover, in group A, the median age and number of women were significantly lower than in the other two groups. It is known that with aging anatomy may change and anatomical relationships in women differ from those in men. However, according to the results of the present study, age and sex did not influence either the clock position or the mutual distances of the splanchnic and the renal vessels at their origin.

It may be interesting to extend the analysis of the cranio-caudal angles of origin of the splanchnic and renal vessels.

CONCLUSIONS

The anatomic variability of origin of both the CT and the SMA from the aorta in terms of the angle from the sagittal aortic plane and mutual distances follows a Gaussian distribution. The same applies to the ostial diameters of renal and visceral vessels. In contrast, the origin of the renal vessels has a statistically significant heterogeneity in terms of angle with the sagittal aortic axis and distance to the SMA, to the aortic bifurcation and between both renal arteries; the variability of these distances and the angle of origin of the LRA correlated with the increase of aortic diameter in the mesenteric and renal aortic region.

According to these results, the main limitation to the manufacture of an “off the shelf” device for the thoracoabdominal aortic region is the large anatomic variability of the renal vessels.

CONFLICT OF INTEREST

None.

FUNDING

None.

REFERENCES

1 Schanzer A, Greenberg RK, Hevelone N, Robinson WP, Eslami MH, Goldberg RJ, et al. Predictors of abdominal aortic aneurysm sac enlargement after endovascular repair. *Circulation* 2011;**123**:2848—55.
2 Park JH, Chung JW, Choo IW, Kim SJ, Lee JY, Han MC. Fenestrated stent-grafts for preserving visceral arterial branches in the treatment of abdominal aortic aneurysms: preliminary experience. *J Vasc Interv Radiol* 1996;**7**:819—23.
3 Svensson LG. Paralysis after aortic surgery: in search of lost cord function. *Surgeon* 2005;**3**:396—405.
4 Scali ST, Feezor RJ, Chang CK, Waterman AL, Berceli SA, Huber TS, et al. Critical analysis of results after chimney endovascular aortic aneurysm repair raises cause for concern. *J Vasc Surg* 2014;**60**:865—74.
5 Katsargyris A, Oikonomou K, Klonaris C, Topel I, Verhoeven EL. Comparison of outcomes with open, fenestrated, and chimney graft repair of juxtarenal aneurysms: are we ready for a paradigm shift? *J Endovasc Ther* 2013;**20**:159—69.
6 Sobocinski J, d'Utra G, O'Brien N, Midulla M, Maurel B, Guillou M, et al. Off-the-shelf fenestrated endografts: a realistic option for more than 70% of patients with juxtarenal aneurysms. *J Endovasc Ther* 2012;**19**:165—72.
7 Bisdas T, Donas KP, Bosiers M, Torsello G, Austermann M. Anatomical suitability of the T-branch stent-graft in patients with thoracoabdominal aortic aneurysms treated using custom-made multibranched endografts. *J Endovasc Ther* 2013;**20**:672—7.
8 Iezzi R, Di Stasi C, Dattesi R, Pirro F, Nestola M, Cina A, et al. Proximal aneurysmal neck: dynamic ECG-gated CT angiography-conformational pulsatile changes with possible consequences for endograft sizing. *Radiology* 2011;**260**:591—8.
9 Iezzi R, Dattesi R, Pirro F, Nestola M, Santoro M, Snider F, et al. CT angiography in stent-graft sizing: impact of using inner vs. outer wall measurements of aortic neck diameters. *J Endovasc Ther* 2011;**18**:280—8.
10 Iezzi R, Santoro M, Dattesi R, La Torre MF, Guerra A, Antonuccio EG, et al. Post-EVAR aortic neck elongation: is a real phenomenon or a conformational change during the cardiac cycle? *Eur Rev Med Pharmacol Sci* 2014;**18**:975—80.